Uncertainty Laws of MIMO Modal Identification

BINBIN LI and PEIXIANG WANG

ABSTRACT

'Uncertainty law' aims at closed-form asymptotic formulas for the relationship between the identification uncertainties of modal properties (e.g., natural frequency, damping ratio) and test configuration (e.g., number and location of shakers/sensors, noise level, data duration). Focusing on the case of experimental modal analysis with multiple-input and multiple-output, the uncertainty laws of modal parameters for well-separated modes are proposed in the paper. Asymptotic expressions for the posterior coefficient of variation of modal parameters are derived via the Fisher information matrix for long data and small damping scenarios. Assumptions and theory are validated using synthetic test data. Governing factors motivated by the theory are investigated, including the equivalent modal signal-to-noise ratio and data duration. The developed uncertainty laws provide a scientific basis for planning and managing identification uncertainties in vibration tests with known multiple-inputs

INTRODUCTION

Modal parameters (e.g., frequency, damping ratio and mode shape) play a key role in the vibration-based structural health monitoring. They can be identified from the recorded structural vibration responses with known input force (i.e., experimental modal analysis, EMA) or without known input force (i.e., operational modal analysis, OMA). No matter known or unknown the input force, the identified modal parameters are subject to uncertainties due to measurement error, modeling error and statistical error. Knowing the identification uncertainty not only gives us the confidence on the identification, but also allows us to make more reliable decisions, e.g., on damage detection and localization.

Focusing on the quantitative calculation of identification uncertainties, various methods have been proposed in the past decades, mainly from the perspective of Bayesian approach [1,2] and frequentist approach [3,4]. Knowing the identification uncertainty is valuable. However, the identification uncertainties are represented by some numerical numbers (e.g., variance), which does not provide any insight into what

Binbin Li, Zhejiang University, 718 Haizhou East Road, Haining, Zhejiang, China
Peixiang Wang, Zhejiang University, 718 Haizhou East Road, Haining, Zhejiang, China

factors it depends on, not to mention any solutions that would help to reduce the uncertainty. To address this problem, 'uncertainty laws' has been recently developed in OMA, aiming at understanding and managing the identification uncertainties of modal properties. Rather than numerical numbers, the uncertainties laws represent the posterior coefficient of variation (c.o.v.) of modal parameters by simple analytical expressions, directly showing how the test configuration influences the identification uncertainty of modal parameters. In particular, References [5] and [6] present uncertainty laws using single-setup and multi-setup FFT data, respectively. Reference [7] illustrates an application of uncertainty laws by proposing metrics to quantify a multi-setup configuration and optimize it accordingly.

In this paper, the uncertainty law for modal identification with known multiple-input multiple-output (MIMO) is developed, i.e., from a perspective of EMA. First, a Bayesian formulation of MIMO modal identification is presented in Section 2, which provides the probabilistic model for the uncertainty law. The main assumptions and key results of uncertainty laws are then discussed in Section 3. A synthetic example is applied in Section 4 for verification of the proposed uncertainties and investigating the key factors. A brief conclusion is finally provided in Section 5.

BAYESIAN MIMO MODAL IDENTIFICATION

Without loss of generality, let $\{\hat{\ddot{\boldsymbol{y}}}_j \in \mathbb{R}^n : j = 0,1,\dots,N-1\}$ be the acceleration time history at n measured degrees of freedom (DoFs) of a structure and $\{\boldsymbol{p}_j \in \mathbb{R}^m : j = 0,1,\dots,N-1\}$ be the input force vector measured at m DoFs, where N is the number of samples per data channel. The scaled FFT $\{\hat{\boldsymbol{Y}}_k\}$ of $\{\hat{\ddot{\boldsymbol{x}}}_j\}$ is defined as

$$\hat{\boldsymbol{Y}}_k = \sqrt{\frac{\Delta t}{N}} \sum_{j=0}^{N-1} \hat{\ddot{\boldsymbol{y}}}_j \exp\left(-\frac{\mathbf{i} 2\pi jk}{N}\right) \ (k = 1,\dots,N) \tag{1}$$

where $\mathbf{i}^2 = -1$ and Δt (sec) is the sampling interval. For $k \le N_q$, $\hat{\boldsymbol{Y}}_k$ corresponds to the frequency $\mathrm{f}_k = k/N\Delta t$ (Hz), where $N_q = \mathrm{int}[N/2] + 1$ ($\mathrm{int}[\cdot]$ denotes the integer part). Similarly, we have the scaled FFT of input force as $\boldsymbol{P}_k$.

Consider identifying a classically damped and well-separated mode on a selected frequency band, the scaled FFT of data within the band is modeled as

$$\hat{\boldsymbol{Y}}_k = \boldsymbol{\varphi}\ddot{\eta}_k + \boldsymbol{\varepsilon}_k \tag{2}$$

where $\boldsymbol{\varphi}$ is the partial mode shape confined to measured DoFs, $\boldsymbol{\varepsilon}_k$ is the scaled FFT of error (e.g., measurement noise and modeling error), and $\ddot{\eta}_k$ is the scaled FFT of the modal response. It is related with the input force $\boldsymbol{P}_k$ as

$$\ddot{\eta}_k = h_k \boldsymbol{\Gamma}^{\mathrm{T}} \boldsymbol{P}_k \tag{3}$$

where the vector $\boldsymbol{\Gamma} = [\Gamma_1,\dots,\Gamma_m]^T \in \mathbb{R}^m$ is the modal participation factor (MPF); h_k is the frequency response function given by

$$h_k = [(1-\beta_k^2) - \mathbf{i}(2\zeta\beta_k)]^{-1};\ \ \beta_k = f/\mathrm{f}_k \tag{4}$$

with f and ζ being the modal frequency and damping ratio, respectively. Substituting Eq. (3) to Eq. (2) gives

$$\hat{\boldsymbol{Y}}_k = \boldsymbol{\varphi} h_k \boldsymbol{\Gamma}^{\mathrm{T}} \boldsymbol{P}_k + \boldsymbol{\varepsilon}_k \tag{5}$$

which directly builds the input-output relationship.

Assuming that the error $\boldsymbol{\varepsilon}_k$ follows a complex normal distribution with zero mean and covariance matrix (a.k.a. power spectral density, PSD) of $S_e\boldsymbol{I}_n$, i.e., $\boldsymbol{\varepsilon}_k \sim \mathrm{CN}(0, S_e\boldsymbol{I}_n)$, and $\boldsymbol{\varepsilon}_j$ is independent of $\boldsymbol{\varepsilon}_k$ for $j \neq k$, it then follows that $\widehat{\boldsymbol{Y}}_k \sim \mathrm{CN}(\boldsymbol{\varphi} h_k \boldsymbol{\Gamma}^{\mathrm{T}} \boldsymbol{P}_k, S_e\boldsymbol{I}_n)$. Here, the input force $\boldsymbol{P}_k$ is assumed to be known without uncertainty. Given the measurement $\{\widehat{\boldsymbol{Y}}_k, k = 1,2,\dots,N_f\}$, where N_f is the number of FFT points within the selected frequency band, one has the negative log-likelihood function (NLLF):

$$L(\boldsymbol{\theta}) = nN_f \ln \pi + nN_f \ln S_e + S_e^{-1} \sum_k \left[\widehat{\boldsymbol{Y}}_k - \boldsymbol{\varphi} h_k \boldsymbol{\Gamma}^{\mathrm{T}} \boldsymbol{P}_k\right]^* \left[\widehat{\boldsymbol{Y}}_k - \boldsymbol{\varphi} h_k \boldsymbol{\Gamma}^{\mathrm{T}} \boldsymbol{P}_k\right] \quad (6)$$

Assuming a uniform prior distribution for unknown parameters $\boldsymbol{\theta} = \{f, \zeta, \boldsymbol{\varphi}, \boldsymbol{\Gamma}, S_e\}$, the posterior probability density function (PDF) can be obtained according to the Bayes' theorem

$$p\left(\boldsymbol{\theta} \middle| \{\widehat{\boldsymbol{Y}}_k\}\right) \propto p\left(\{\widehat{\boldsymbol{Y}}_k\} \middle| \boldsymbol{\theta}\right) = e^{-L(\boldsymbol{\theta})} \quad (7)$$

Note that one can obtain identical NLLFs when multiplying $\boldsymbol{\varphi}$ by a constant c and then dividing it by $\boldsymbol{\Gamma}$, because $\boldsymbol{\varphi}\boldsymbol{\Gamma}^{\mathrm{T}} = (c\boldsymbol{\varphi})(\boldsymbol{\Gamma}^{\mathrm{T}}/c)$, which indicates that the formulated problem is actually unidentifiable. To make the parameters (locally) identifiable, a norm constraint of $\boldsymbol{\varphi}^{\mathrm{T}}\boldsymbol{\varphi} = 1$ is further introduced here. The analytical form of posterior PDF $p\left(\boldsymbol{\theta} \middle| \{\widehat{\boldsymbol{Y}}_k\}\right)$ does not exist due to the complicated nature of NLLF. With sufficient data, Laplace approximation is adopted, i.e., fitting the posterior PDF with a multivariate normal distribution, whose mean vector and covariance matrix are, respectively, given by

$$\widehat{\boldsymbol{\theta}} = \arg\min_{\boldsymbol{\theta}} L(\boldsymbol{\theta}); \quad \widehat{\boldsymbol{\Sigma}} = \left[\left.\frac{\partial^2 L(\boldsymbol{\theta})}{\partial \boldsymbol{\theta} \partial \boldsymbol{\theta}^{\mathrm{T}}}\right|_{\boldsymbol{\theta}=\widehat{\boldsymbol{\theta}}}\right]^{-1} \quad (8)$$

where the operator '$\arg\min_{\boldsymbol{\theta}}[\cdot]$' denotes the value of $\boldsymbol{\theta}$ that minimizes NLLF $L(\boldsymbol{\theta})$. The mean $\widehat{\boldsymbol{\theta}}$ is often called the most probable value (MPV) in Bayesian modal identification. The covariance matrix $\widehat{\boldsymbol{\Sigma}}$ is the inverse of the Hessian of the NLLF at the MPV, which quantifies the remaining uncertainties of modal parameters. For simplicity, the above Bayesian MIMO modal identification algorithm will be referred as 'BAYEMA' (Bayesian experimental modal analysis) in the paper.

OVERVIEW OF UNCERTAINTY LAWS

Within the context of Bayesian MIMO modal identification, the mode of interest is assumed to be well-separated from others and with natural frequency f (in Hz), damping ratio ζ and normalized mode shape $\boldsymbol{\varphi}$. The structure is subject to an input force vector $\boldsymbol{P}_k$ with an MPF $\boldsymbol{\Gamma}$. The selected frequency band for dentification is assumed to be $f(1 \pm \kappa\zeta)$, where κ is a dimensionless bandwidth factor. Assuming the sampling duration is T_d, one has the effective data length $N_c = T_d f$ and the number of FFT points $N_f = 2\kappa\zeta f T_d$ within the selected frequency band.

Based on the above assumptions, it can be shown that for long data $N_f \gg 1$ and small damping $\zeta \ll 1$, the (squared) posterior coefficient of variation (c.o.v. = standard deviation/mean) δ_x^2 of the modal parameter x is asymptotically given by

$$\delta_x^2 \sim \delta_{x,mimo}^2 = \delta_{x0}^2 \frac{b_x}{\gamma} \qquad \text{for } N_f \gg 1, \zeta \ll 1 \quad (9)$$

where $\delta_{x,mino}^2$ is referred as the uncertainty laws of MIMO modal identification. The operator '$\sim$' denotes that the ratio of the two sides tends to 1 under the asymptotic conditions. The corresponding expressions of δ_{x0}^2 and b_x are shown in Table 1. Here, δ_{x0}^2 (except for mode shape and modal participation factor) is the 'zeroth order law' of OMA [8], and b_x is defined to be the 'known-input factor', showing how the squared c.o.v. reduces with known multiple-input.

$$\gamma = \frac{S_\Gamma}{4S_e\zeta^2} \tag{10}$$

is defined to be the (dimensionless) 'modal s/n ratio', where $S_\Gamma = \boldsymbol{\Gamma}^{\mathrm{T}}\mathrm{Re}(\boldsymbol{S})\boldsymbol{\Gamma}$ is the modal force PSD and

$$\boldsymbol{S} = N_f^{-1}\sum\nolimits_{N_f}\boldsymbol{P}_k\boldsymbol{P}_k^* \tag{11}$$

is the PSD of the input force $\boldsymbol{P}_k$. The input force PSD $\boldsymbol{S}$ is assumed to be constant within the selected frequency band.

The expressions of δ_{x0}^2 and b_x for different parameters are summarized in Table I. The uncertainty laws capture the leading order behavior of posterior c.o.v.s of modal parameters under asymptotic conditions, i.e., $\delta_x^2/\delta_{x,mimo}^2 \to 1$ as for $N_f \gg 1$ and $\zeta \ll 1$. The derivation take advantages of long data asymptotics, small damping asymptotics and asymptotic decoupling [8]. Due to the space limit, the detailed derivation of uncertainty laws shown in Table 1 is ignored, but an empirical verification is provided in the next section.

TABLE I. KEY RESULTS OF UNCERTAINTY LAWS

Parameter x	**zeroth order law δ_{x0}^2 ***	**Data length factor $B_x(\kappa)$**	**Known-input factor $b_x(\kappa)$**
Frequency f	$\frac{\zeta}{2\pi N_c B_f}$	$\frac{2}{\pi}\left(\tan^{-1}\kappa - \frac{\kappa}{\kappa^2+1}\right)$	$\frac{2\left(\tan^{-1}\kappa - \frac{\kappa}{\kappa^2+1}\right)}{\tan^{-1}\kappa + \frac{\kappa}{\kappa^2+1}}$
Damping ζ	$\frac{1}{2\pi\zeta N_c B_\zeta}$	$\frac{2}{\pi}\left[\tan^{-1}\kappa + \frac{\kappa}{\kappa^2+1} - \frac{2(\tan^{-1}\kappa)^2}{\kappa}\right]$	$\frac{4\tan^{-1}\kappa\left[\tan^{-1}\kappa + \frac{\kappa}{\kappa^2+1} - \frac{2(\tan^{-1}\kappa)^2}{\kappa}\right]}{\left(\tan^{-1}\kappa + \frac{\kappa}{\kappa^2+1}\right)\left(\tan^{-1}\kappa - \frac{\kappa}{\kappa^2+1}\right)}$
Mode shape $\bar{\boldsymbol{\varphi}}$	$\frac{n-1}{2\pi\zeta N_c B_{\bar{\varphi}}}$	$\frac{2}{\pi}\tan^{-1}\kappa$	1
Modal participation factor Γ_i	$\frac{1}{2\pi\zeta N_c B_\Gamma}$	$\frac{2}{\pi}\tan^{-1}\kappa$	$\frac{S_\Gamma}{\Gamma_i^2 P_{ii}^{-1}} + \frac{tan^{-1}\kappa + \frac{\kappa}{\kappa^2+1}}{tan^{-1}\kappa - \frac{\kappa}{\kappa^2+1}}$
Channel noise PSD S_e	$\frac{1}{(n-1)N_f B_{S_e}}$	1	$\frac{n-1}{n}\gamma$

Note: Symbols $f, \zeta, \boldsymbol{\varphi}, \boldsymbol{\Gamma}, S_e$ here denote the 'true' value of modal properties rather than the variable in the likelihood function.
Effective data length N_c = data length/natural period; $\gamma = S_\Gamma/4S_e\zeta^2$ is the modal s/n ratio;
Mode shape c.o.v. is defined as the square root sum of eigenvalues of the covariance matrix of $\boldsymbol{\varphi}$;
$\boldsymbol{P} = \mathrm{Re}(\boldsymbol{S})^{-1}$ and P_{ii} represents the correponding i-th diagonal entry;
The selected band for modal identification is $f(1 \pm \kappa\zeta)$ where κ is the bandwidth factor.
* δ_{x0}^2 coincides with the 'zeroth order law' of OMA when x is f, ζ or S_e.

EMPIRICAL VERIFICATION

An example is presented with synthetic data to verify the proposed uncertainty laws. The considered structure is a three-story shear-type building, as depicted in Figure 1(a). The building is of 600 mm high with each floor measuring 200 mm × 100 mm × 8 mm. The first two modes with 1% damping ratio have the natural frequencies of 1.976 Hz and 2.617 Hz, respectively. Two input forces have been applied on the top floor along the weak and strong direction. They are modeled by stationary Gaussian white noise with identical PSD but with varying coherence. Acceleration time history along the two directions at each node is recorded for investigation, yielding the total number of measured DoFs is $4 \times 2 \times 3 = 24$. Synthetic acceleration data is generated at a sampling rate of 100 Hz. The duration of measured acceleration is 600 sec, which covers 10 sec before the excitations are applied, 580 sec pseudorandom excitation, and 10 sec free vibration after the excitations are applied. The measurement noise is modeled by a stationary Gaussian white noise process with a PSD of $S_e = 1 \times 10^{-6}$ g^2/Hz. In this example, it is assumed the external mass is 1 kg.

Two cases are investigated with a brief description summarized in Table II. Case 1 shows the effect of modal s/n ratio on identification uncertainty due to different magnitudes of excitations. Case 2 shows the effect of effective data length (measurement duration/natural period). The data generated in both cases is used for a direct verification of uncertainty laws. The PSD of input forces and root singular value (SV) spectrum of output responses are shown in Figure 1(c)~(d) for a typical realization.

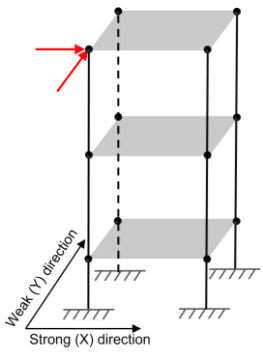

a) Test configuration
(arrows: excitations; dot: biaxial accelerometer)

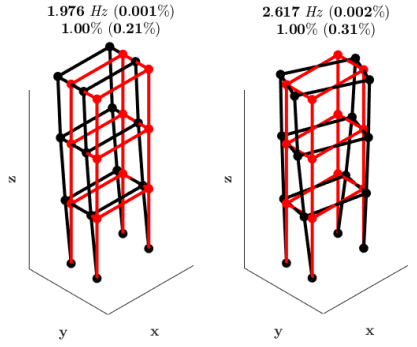

b) Identified results, Mode TY1, Mode R1

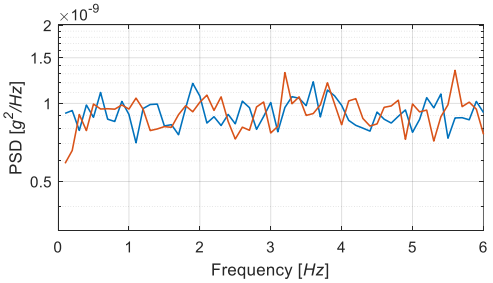

c) Typical PSD of input

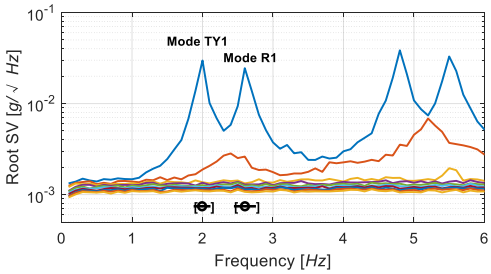

d) Typical Root SV of output

Figure 1. three-story shear-type building, synthetic data

TABLE II .TEST CONFIGURATION, SYNTHETIC DATA

Case ID	Force PSD ($\times 10^{-6}$ N^2/Hz)	Data duration (sec)
1	$\boldsymbol{S} = \begin{bmatrix} \alpha & 0 \\ 0 & \alpha \end{bmatrix}$ with $\alpha = 0.1{:}\,0.1{:}\,1$	600
2	$\boldsymbol{S} = \begin{bmatrix} 1 & 0 \\ 0 & 1 \end{bmatrix}$	From 60 to 1140 with a interval of 120

The initial guesses of frequencies and bands for modal identification are indicated with circles and brackets in the SV spectrum. The BAYEMA algorithm is then applied to identify the first two vibration modes. Identified results are illustrated in Figure 1(b). Natural frequencies and damping ratios are depicted with their uncertainties in parentheses.

Direct Verification

The derived uncertainty laws are first verified by comparing the identification uncertainties calculated by BAYEMA predicted by the corresponding uncertainty laws, as shown in Figure 2. It is observed that all markers are distributed around the diagonal lines, indicating a good agreement between BAYEMA and uncertainty laws. One can see the developed uncertainty laws can capture the identification uncertainty of modal parameters with simple analytical expressions. It should be noted that for Mode TY1, which is the first transverse mode along the weak direction, modal participation factor along the strong direction is purely zero. Therefore, its coefficient of variation does not exist and is not considered here.

Effect of Modal S/N Ratio

For Case 1, the effect of modal s/n ratio on identification uncertainty is investigated, which is implemented by varying the magnitude of input force. In addition to the proposed uncertainty law, results of uncertainty law of OMA [5] and BAYOMA [9] are also provided to illustrate the benefit of knowing the input force. The resulting posterior c.o.v.s of the identified modal parameters are shown in Figure 3, where circle and cross markers represent results of BAYEMA and BAYOMA respectively, while dashed and solid lines show the value predicted by uncertainty laws for known and unknown-input cases, respectively.

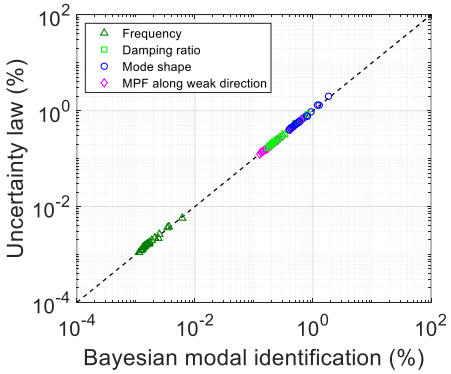

a) Mode TY1

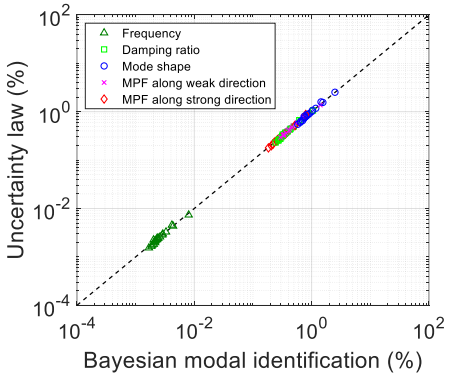

a) Mode R1

Figure 2. Posterior c.o.v. calculated by BAYEMA versus uncertainty laws

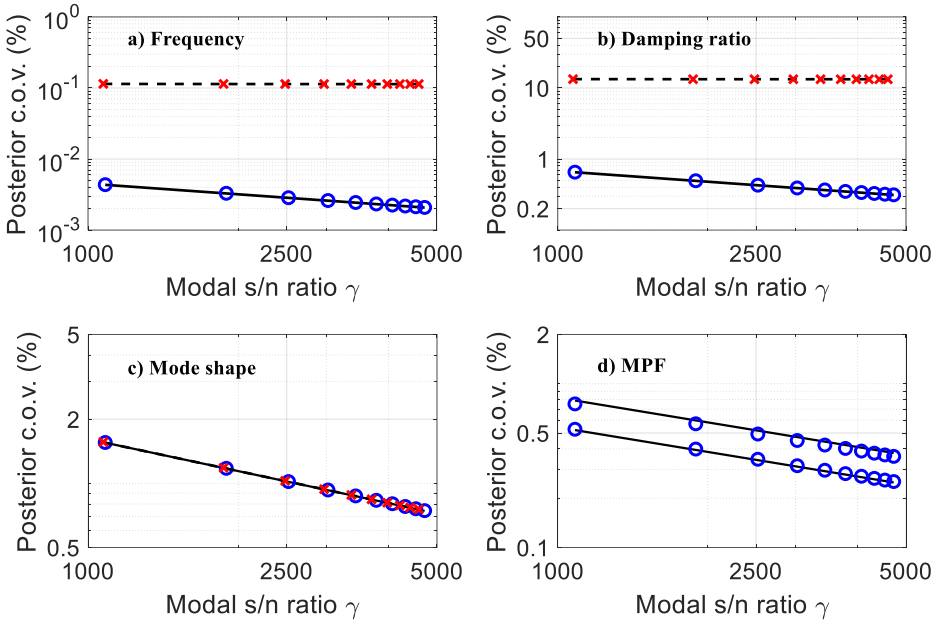

Figure 3. Effect of modal s/n ratio on posterior c.o.v. of modal parameters; Mode R1.
(Circle: identified value with known input; Cross: identified value with unknown input; Solid line: uncertainty laws with known input; Dashed line: uncertainty laws with unknown input)

As depicted in Figure 3, the posterior c.o.v.s of the identified modal parameters decrease as γ increases regardless of whether the input is known or not. Compared to unknown-input case, the identification uncertainty in the known-input case is mainly governed by channel noise, which can be reduced effectively by increasing γ and finally it could be close to zero for a large enough value of γ.

Effect of Data Length

We next investigate the influence of effective data length N_c. From the uncertainty law formula, it is observed that with the increase of N_c, the posterior c.o.v.s decrease. In this context, extending the test duration is one of simple ways to reduce the identification uncertainty. Verified by Figure 4, the c.o.v.s decrease in a vanishing manner with increasing N_c.

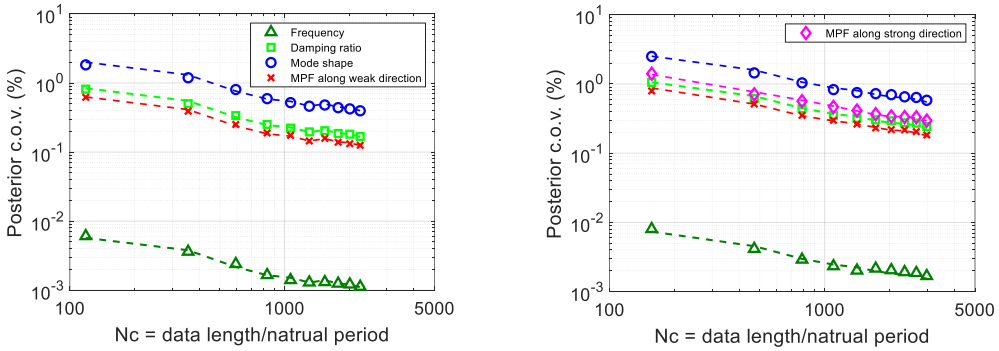

a) Mode TY1 b) Mode R1

Figure 4. Effect of effective data length on posterior c.o.v. of modal parameters.
(Marker: identified value with known input; Dashed line: uncertainty laws with known input)

CONCLUSION

This paper develops the closed-form asymptotic expressions, i.e., uncertainty laws, for the identification uncertainty of modal parameters with known broadband input. They are derived for a well-separated mode with assumptions of small damping ratio and long data. Synthetic data are used to verify the accuracy of uncertainties, and a parametric study is conducted to investigate the key factors. Key results of uncertainty laws show the beauty of nature, i.e., remarkably simple and insightful expressions dominate the identification uncertainty of modal parameters. The derived uncertainty laws allow us to understand how the identification uncertainty depends on test configuration, and thus provides an opportunity to optimize the test configuration for a more precise estimation.

REFERENCES

1. Au SK, Zhang FL. On assessing the posterior mode shape uncertainty in ambient modal identification. *Probabilistic Engineering Mechanics* 2011; **26**(3): 427–434. DOI: 10.1016/j.probengmech.2010.11.009.
2. Au SK. Fast Bayesian ambient modal identification in the frequency domain, Part II: Posterior uncertainty. *Mechanical Systems and Signal Processing* 2012; **26**: 76–90. DOI: 10.1016/j.ymssp.2011.06.019.
3. Reynders E, Pintelon R, De Roeck G. Uncertainty bounds on modal parameters obtained from stochastic subspace identification. *Mechanical Systems and Signal Processing* 2008; **22**(4): 948–969. DOI: 10.1016/j.ymssp.2007.10.009.
4. Lam XB, Mevel L. Uncertainty Quantification for Eigensystem-Realization-Algorithm, A Class of Subspace System Identification. *IFAC Proceedings Volumes* 2011; **44**(1): 6529–6534. DOI: 10.3182/20110828-6-IT-1002.00619.
5. Au SK. Uncertainty law in ambient modal identification—Part I: Theory. *Mechanical Systems and Signal Processing* 2014; **48**(1–2): 15–33. DOI: 10.1016/j.ymssp.2013.07.016.
6. Xie YL, Au SK, Li B. Asymptotic identification uncertainty of well-separated modes in operational modal analysis with multiple setups. *Mechanical Systems and Signal Processing* 2021; **152**: 107382. DOI: 10.1016/j.ymssp.2020.107382.
7. Li B. Measuring configuration of multi-setup ambient vibration test. *Mechanical Systems and Signal Processing* 2022.
8. Au SK. *Operational Modal Analysis*. Singapore: Springer; 2017. DOI: 10.1007/978-981-10-4118-1.
9. Au SK. Fast Bayesian FFT Method for Ambient Modal Identification with Separated Modes. *Journal of Engineering Mechanics* 2011; **137**(3): 214–226. DOI: 10.1061/(ASCE)EM.1943-7889.0000213.